SUPPLEMENTARY MATERIAL

1 DETAILS OF METHODS

1.1 Equations for the deterministic discrete trait variation model

In Table 1 of the main text, we presented equations for the deterministic trait variation model when the trait sapling mortality rate (μ_i) was variable. Below, we show equations for the model considering other two trait variations:

For varying tree death rate ν_i, there are $2k+1$ coupled differential equations given by:

$$\frac{dS_i}{dt} = \beta G T_i - \omega(G;\theta)S_i - \mu S_i \tag{5}$$

$$\frac{dT_i}{dt} = \omega(G;\theta)S_i - \nu_i T_i \tag{6}$$

$$\frac{dG}{dt} = 1 - \sum_i^k (\frac{dS_i}{dt} + \frac{dT_i}{dt}) = \mu S + (\sum_i^k p_i \nu_i)T - \beta GT \tag{7}$$

And similarly for varying half saturation of the fire resistance function θ_i, the $2k+1$ coupled differential equations given by:

$$\frac{dS_i}{dt} = \beta G T_i - \omega(G;\theta_i)S_i - \mu S_i \tag{8}$$

$$\frac{dT_i}{dt} = \omega(G;\theta_i)S_i - \nu T_i \tag{9}$$

$$\frac{dG}{dt} = 1 - \sum_i^k (\frac{dS_i}{dt} + \frac{dT_i}{dt}) = \mu S + \nu T - \beta GT \tag{10}$$

It is also possible to vary more than one trait in which case the type of savanna sapling/tree can be denoted by a vector as in $S_{i,j,l}$ or $T_{i,j,l}$ and the sum is over all such tuples. The system of $2k_1 k_2 k_3 + 1$ equations would then be, for example:

$$\frac{dS_{i,j,l}}{dt} = \beta G T_i - \omega(G;\theta_l)S_{i,j,l} - \mu_i S_{i,j,l} \tag{11}$$

$$\frac{dT_{i,j,l}}{dt} = \omega(G;\theta_l)S_{i,j,l} - \nu_j T_{i,j,l} \tag{12}$$

$$\frac{dG}{dt} = 1 - \sum_{l=1}^{k_3} \sum_{j=1}^{k_2} \sum_{i=1}^{k_1} (\frac{dS_{i,j,l}}{dt} + \frac{dT_{i,j,l}}{dt}) = (\sum_{i=1}^{k_1} p_i \mu_i)S + (\sum_{j=1}^{k_2} p_j \nu_j)T - \beta GT \tag{13}$$

1.2 Simulation details of the deterministic trait variation model

For the no variation case, we use analytical methods to find the equilibrium grass and tree cover (using Wolfram Research, Inc., Mathematica, Version 12.2).

For the deterministic discrete trait variation model, we numerically integrate the system of ordinary differential equations using Euler's method. For each value of sapling birth rate (β), we run the simulations with various initial values of the grass cover: $G_0 = 0, 0.1, 0.2,..,$ or 0.9. For a given G_0, we set both the overall initial tree and sapling cover to be equal to $(1-G_0)/2$. Using this initial proportion cover of tree (and sapling), we assume that this proportion is distributed equally among all corresponding k types, i.e., each sapling or tree type has a proportion cover of $(1-G_0)/2k$.

For each parameter value, we run the simulations for 10^7 time steps, with a step size of 0.001. We observe that the system reaches steady-state much earlier, typically by 10^5 time steps, as seen in Fig 4A of the main text.

To better understand the mechanisms at play, we study the population level dynamics wherein we examine how the covers of all variables (G, S_1, S_2,...,S_{10}, T_1, T_2,...,T_{10}) change with time in all these cases.

Low trait variation is implemented as a smaller range of the trait values (0.3 to 0.7) while the*high trait variation* corresponds to a larger range (0 to 1). We present our main text results of the deterministic model for a fixed number of trait-types ($k = 10$). For example, if k was 10 with low trait variation, the specific trait values considered are 0.32, 0.36, 0.4, to 0.68 at an interval of 0.04 units. Note that we also consider $k = 100$ and 1000 and present those results in the Supplementary Materials.

1.3 Some general comments on our discrete trait modelling assumptions and approach

We note that the inheritance in our model is clonal and thus the heritability value is 1. Selection forces for the traits sapling death rate (μ) and tree death rate (ν) are frequency independent as can be seen by looking at the expression of per-capita growth rate; to see this, note that the mortality term for sapling via the equation for per-capita growth rate $\frac{1}{S_i}\frac{dS_i}{dt}$ is equal to μ_i and does not depend on the frequencies of any of the vegetation frequencies. Likewise, the mortality term for savanna trees via the equation for per-capita growth rate $\frac{1}{T_i}\frac{dT_i}{dt}$ is equal to ν_i and does not depend on any of the vegetation frequencies.

One could consider alternative modelling strategies such as game theory or equivalently the replicator equations, or adaptive dynamics. Deriving an expression of the fitness of a type would require casting these equations in the form of a replicator-like equation for the frequency of traits. However, that may not very straightforward due to the structure of the Staver and Levin (2012) model equations we begin with, which are also partly age-structured. However, these are worthwhile alternative modelling approaches that future studies can take. A main advantage of our approach is that in the limit of only one trait, we revert to the well-known model of savanna-woodland-forest dynamics by Staver and Levin (2012), which also serves as no-variation baseline for our analysis.

1.4 Simulation details of the stochastic agent-based model

For the stochastic continuous trait agent-based model, we study the ecosystem-level dynamics in a similar way as for the deterministic model. We look at the changes in the bifurcation diagram with an increase in trait variations. Since this is a stochastic simulation, a single realization is not sufficient to fully understand it. Therefore, for each value of the drive sapling birth rate β (the x-axis of the bifurcation diagram), we simulate the system 1000 times with different initial conditions, take the final state after 1000 time units, and plot a histogram. Each of the simulations starts-off with each of the sapling and tree individuals having a different trait, randomly drawn from a uniform distribution with limits given by the extent of trait variation. The parameter values are used are the same as that of the deterministic model with discrete traits.

Likewise, in the population level dynamics, we look at the dynamics in the trait distribution of a single population. We compare the initial and final distribution of traits for different levels of trait variation. We take the average of the final distribution after 10^4 time units over an ensemble of simulations (10^4 in number) as the process is stochastic.

2 ROBUSTNESS OF RESULTS WITH THE INCLUSION OF FOREST TREE AS A NEW VEGETATION TYPE

To the base model, we add another state variable F, representing forest trees, as in (Staver and Levin, 2012) while incorporating trait variations within S and T traits as before. Note that forest trees are fundamentally different from savanna trees. While savanna trees are fire resistant, forest trees succumb to fire, the impact of which is is captured by a nonlinear sigmoidal like function of $\phi(G)$ which is similar to a mirror image of $\omega(G,\theta)$ (i.e., lower mortality at lower values of G and higher mortality at higher values of G; note that the grass cover implicitly captures the probability or rate of fire in the model). Further, forest trees essentially are an invasive type, competitively excluding all the other functional types; we denote their birth rate by α. The system can be represented by $2k+2$ equations, for instance if the trait being varied was θ:

$$\frac{dG}{dt} = \mu S - \nu T - \phi(G)F + \beta GT - \alpha GF \tag{14}$$

$$\frac{dS_i}{dt} = \beta GT_i - \omega(G;\theta_i)S_i - \mu S_i - \alpha S_i F \tag{15}$$

$$\frac{dT_i}{dt} = \omega(G;\theta_i)S_i - \nu T_i - \alpha TiF \tag{16}$$

$$\frac{dF}{dt} = [\alpha(1-F) - \phi(G)]F \tag{17}$$

where S and T are equal to $\sum_{i=1}^{k} S_i$ and $\sum_{i=1}^{k} T_i$ respectively, $\omega(G;\theta)$ is defined as before and $\phi(G;\theta)$ is defined as:

$$\phi(G) = \phi_0 + \frac{\phi_1 - \phi_0}{1 + e^{(-G+0.5)/s}} \tag{18}$$

where unlike in the case of ω, $\phi_1 > \phi_0$

This system shows rich behavior in terms of bifurcation with respect to multiple parameters (Supplementary figure S11). What is most apparent is that although the grassland-savanna dynamics remain similar, the existence of the woodland state (consisting of savanna saplings and trees) is confined only to parameter ranges with extremely low values of α. For most parameter sets, the low grass cover branch of the bistable region represents invasion by forest trees. Although the original model shows other kinds of behaviors as well such as a coexistence state of all four types which undergoes a Hopf bifurcation with respect to α to become a stable limit cycle, these are for very small parameter ranges very different from that used in our study and therefore we do not consider these.
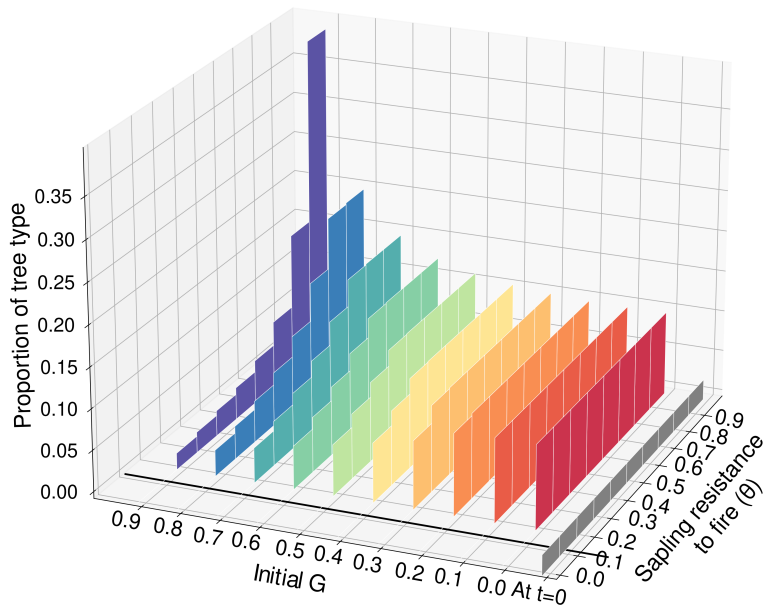
3 SUPPLEMENTARY FIGURES
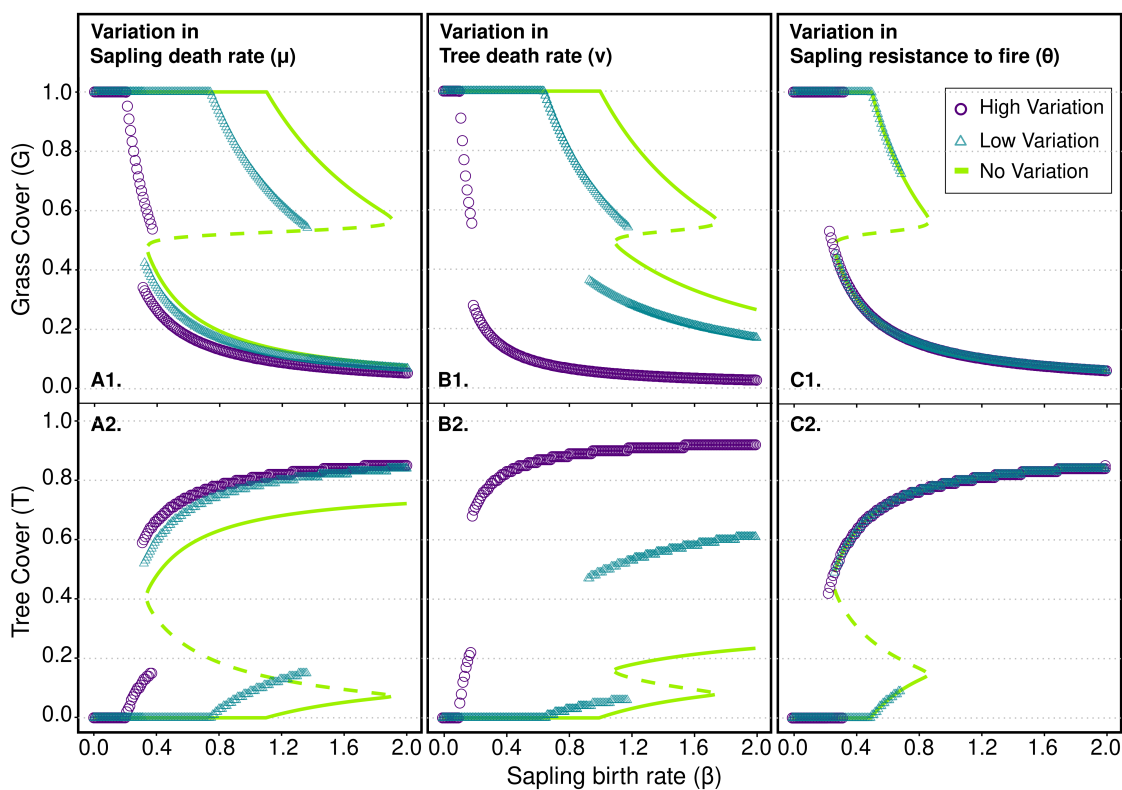
Supplementary Figure S1. For an initial trait distribution following a unimodal beta distribution, we again observe that trait variations alter the properties of bistable regions and regime shifts in a woodland-savanna model. Top row (A1,B1,C1) represents the steady-state grass cover, while the bottom row (A2,B2,C2) represents the steady-state tree cover. Methods and results are same as those of Figure 2 in main text.
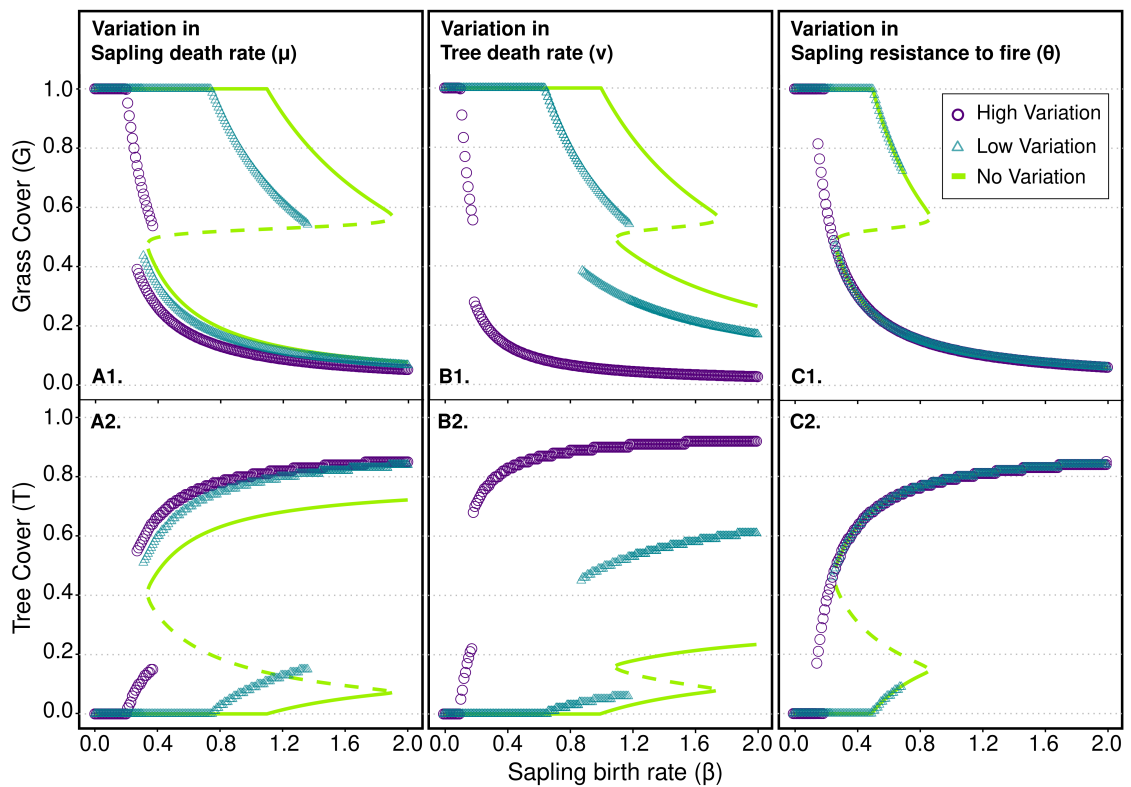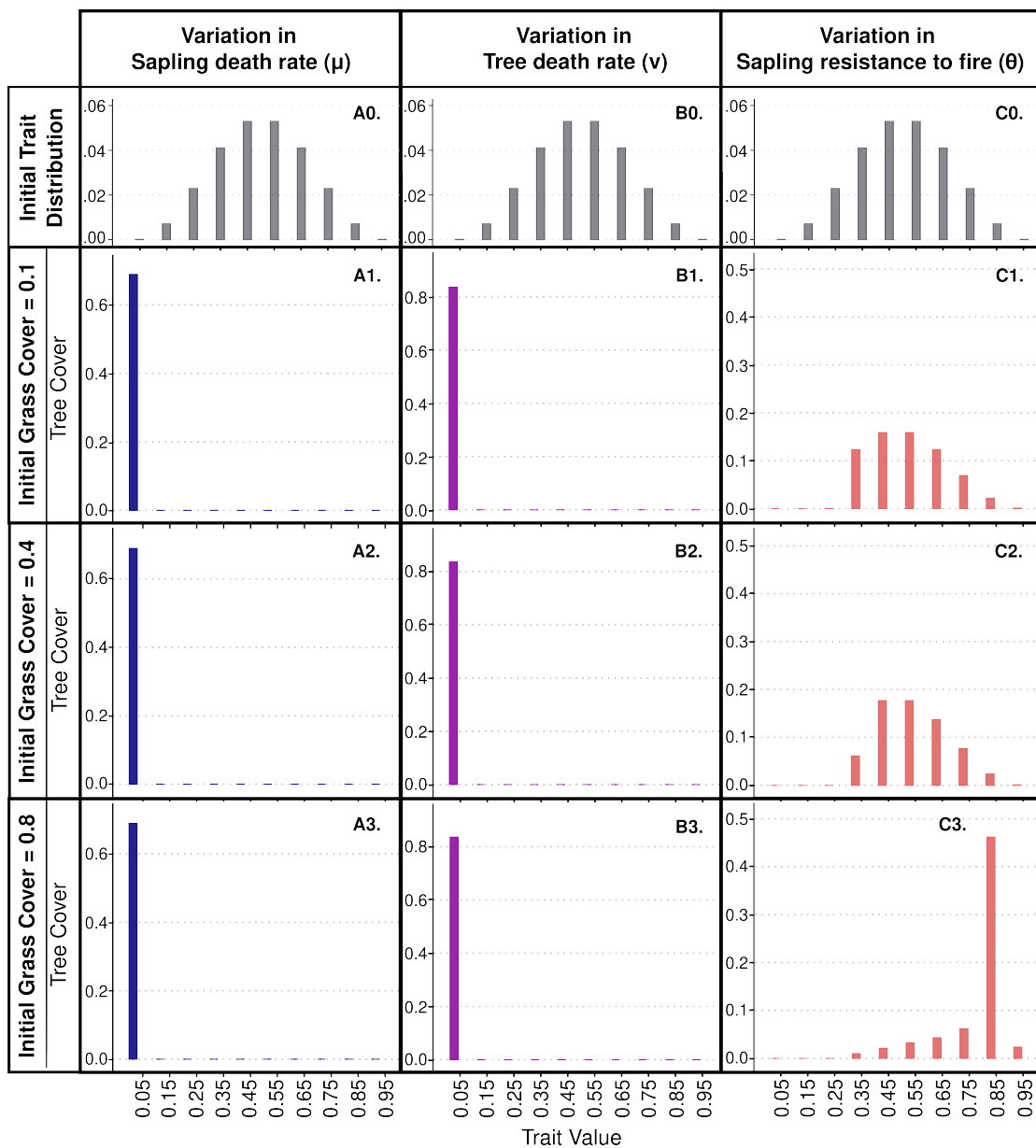
Supplementary Figure S2. For an initial trait distribution following a bimodal beta distribution, we again observe that trait variations alter the properties of bistable regions and regime shifts in a woodland-savanna model. Top row (A1,B1,C1) represents the steady-state grass cover, while the bottom row (A2,B2,C2) represents the steady-state tree cover. Methods and results are same as those of Figure 2in main text
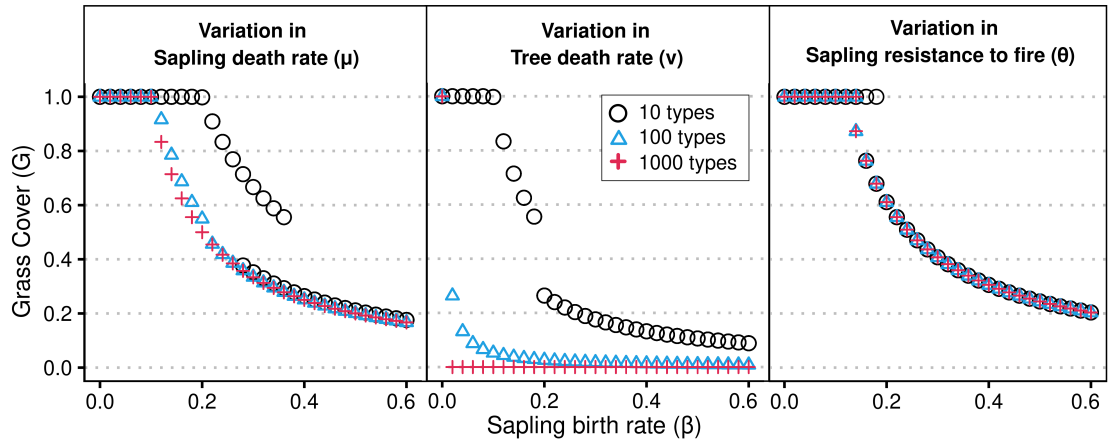
Supplementary Figure S3. Increasing the number of trait types (k) has different effects on the properties of bistable regions and regime shifts for variation in different traits in a woodland-savanna model. We vary the number of trait types (k): 1000 (black circles), 100 (blue triangles) and 10 (pink plus symbol), for each case of variation in a trait while keeping the trait range 0 to 1 (high trait variation), with equally spaced discrete values. As the number of trait types increase, we observe that: (i) the width of bistable region reduces for all cases of trait variations, (ii) the grassland state exists for a smaller range of sapling birth rate (β) for all three cases (iii) the quantum of shift decreases with variation in μ and θ, but increases with variation in ν, (iv) the nature of transitions varies between trait variations. With increasing k, variation in μ and θ result in gradual transition from a woodland to a savanna and then to a grassland state, while variation in ν results in an abrupt transition from a woodland to a grassland state, instead of woodland to savanna state. All parameters except the trait range are the same as for Figure 2.


Supplementary Figure S4. Sensitivity of steady-state distribution of trait values to a range of initial conditions, for β=0.45 which corresponds to the monostable woodland regime. Tree population at the start of the simulation (at t=0, gray bars) consists of 10 θ types present in equal proportion. Bars with the same color correspond to a specific case of initial grass cover, G_0. Steady-state grass cover (G^*) is shown with solid black line. Each bar corresponds to the proportion cover of the tree with the specific value of θ at the steady state. We show how the uniform initial trait distribution evolves for different initial values of grass cover (G_0), while assuming Initial tree and sapling cover are both equal to $(1 - G_0)/2$. For variation in sapling resistance to fire (θ), we find that: (i) tree types with θ less than a threshold value get eliminated from the population, (ii) mean value of the trait at steady state increases with G_0, such that the steady-state population consists of more fire-tolerant individuals.

Supplementary Figure S5. Population-level dynamics for a system with trait values taken from a unimodal beta distribution also show sensitivity to initial conditions, for $\beta = 0.45$ which corresponds to monostable woodland regime. Methods and results are same as those of Figure 3 in main text
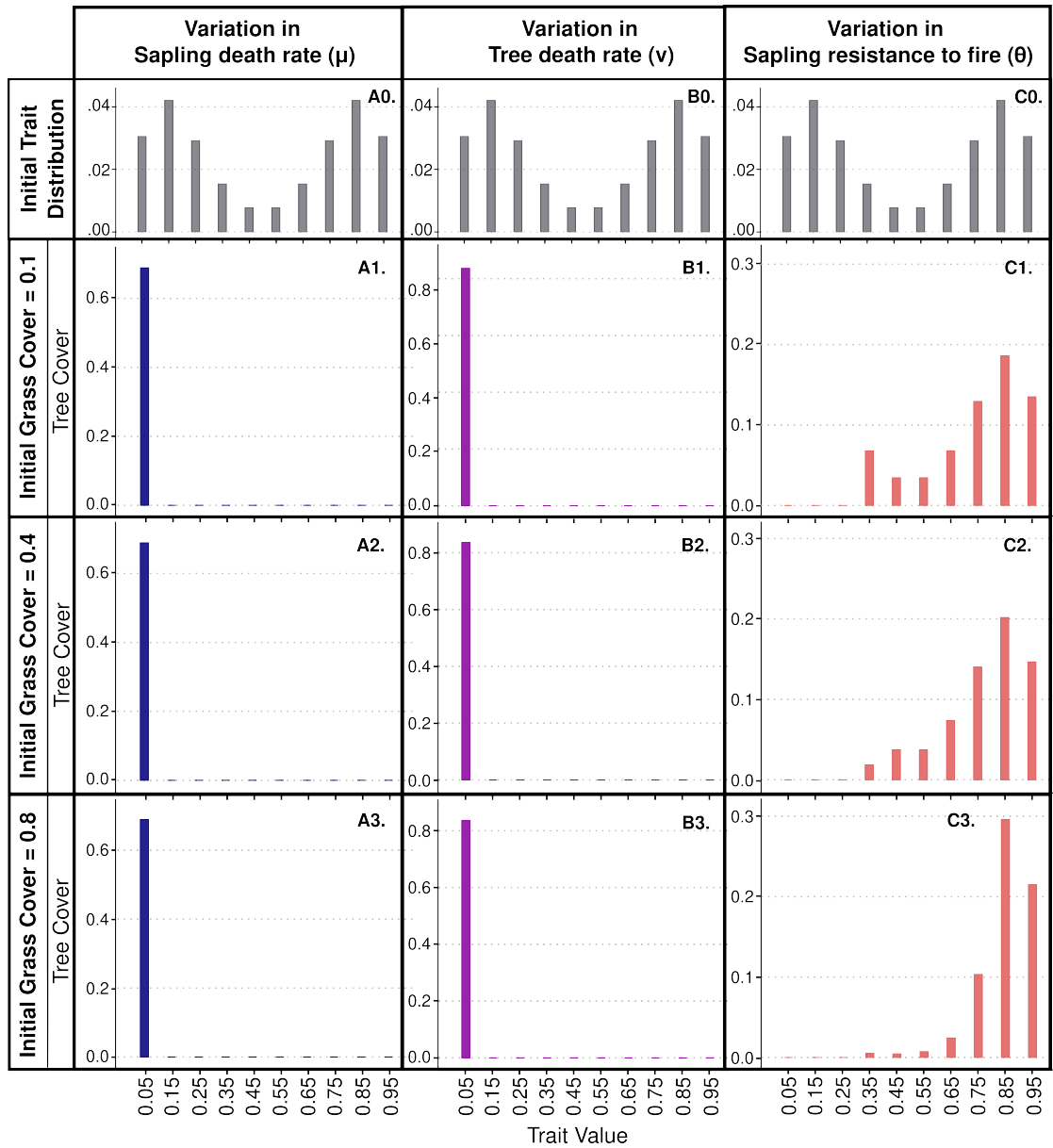
Supplementary Figure S6. Population-level dynamics for a system with trait values taken from a bimodal beta distribution also show sensitivity to initial conditions, for $\beta = 0.45$ which corresponds to monostable woodland regime. Methods and results are same as those of Figure 3 in main text
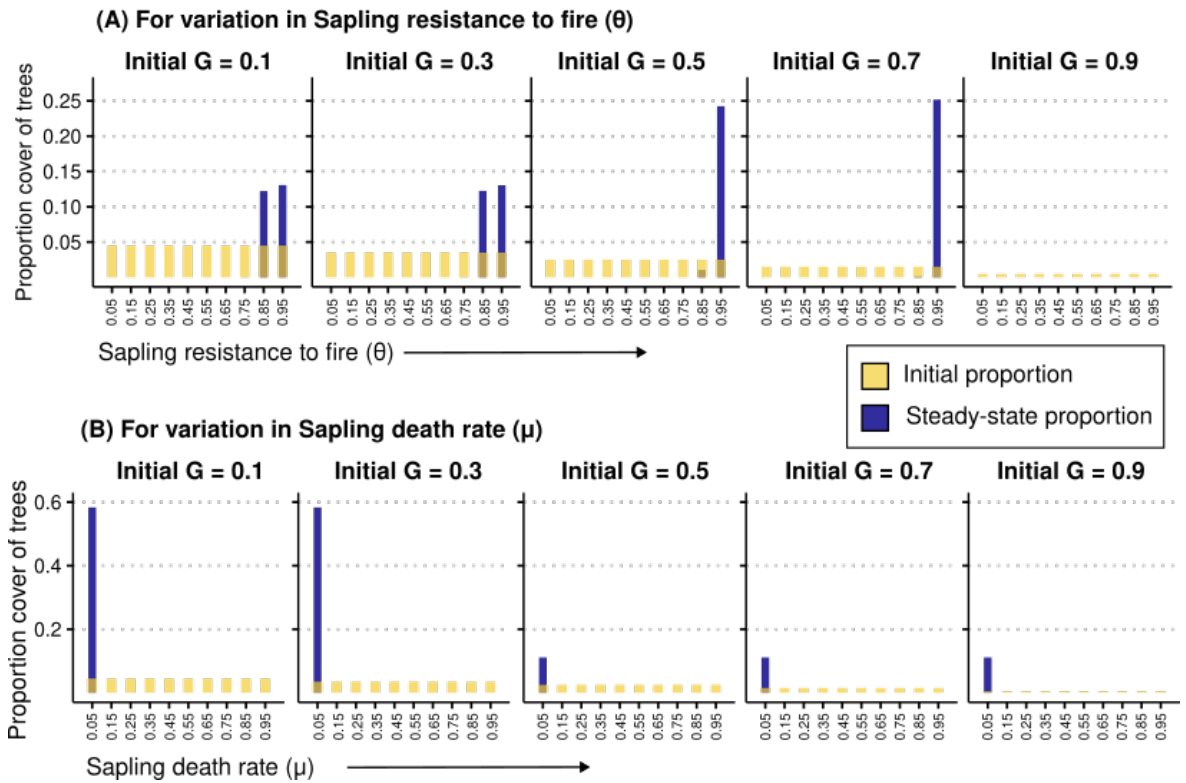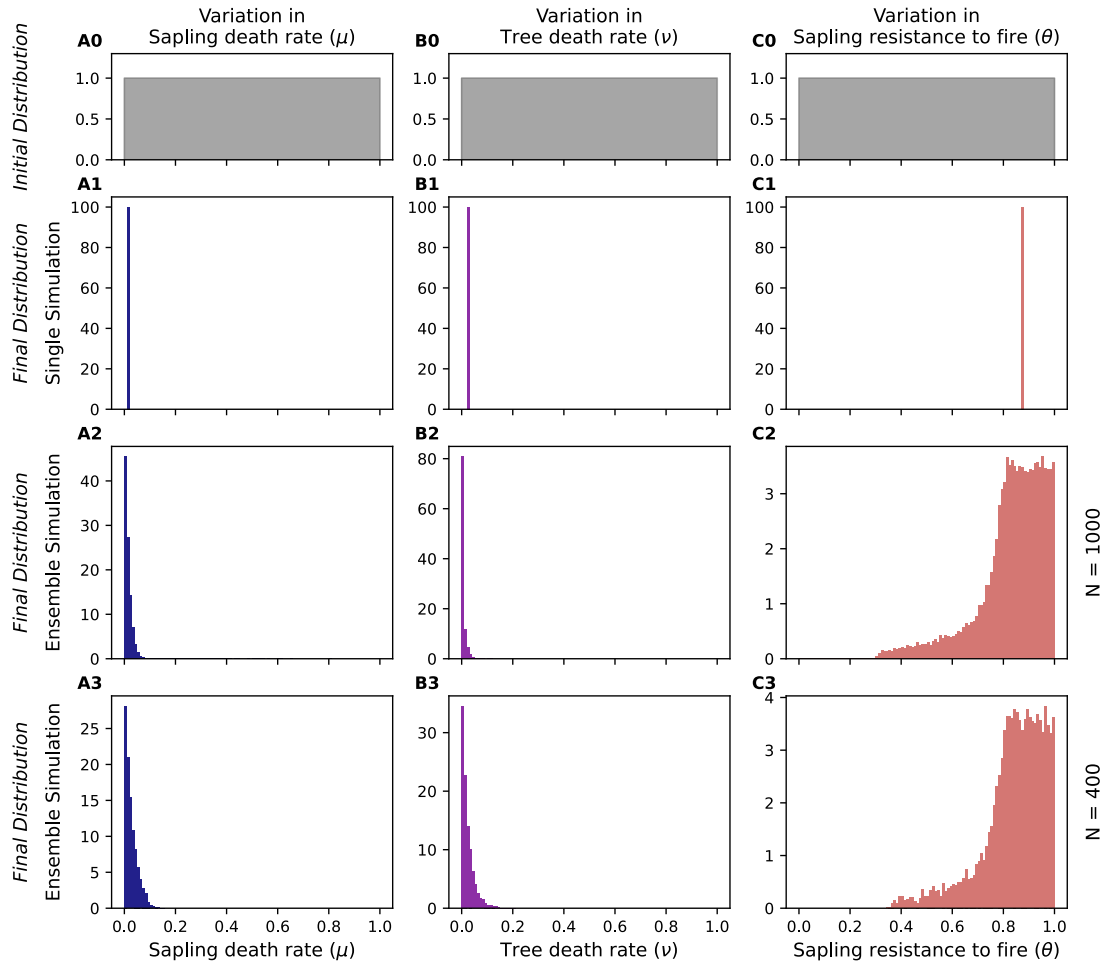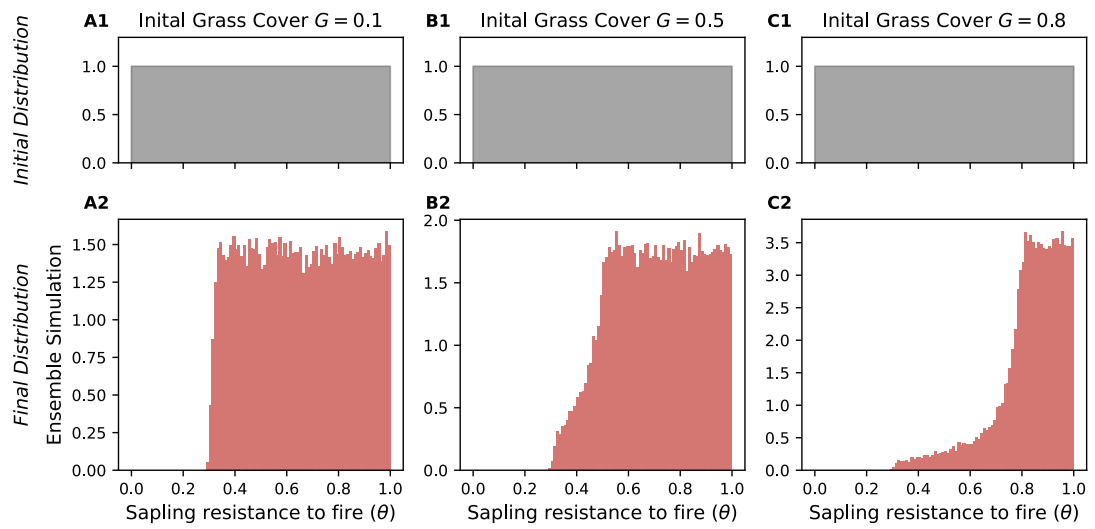
Supplementary Figure S7. Population-level dynamics in the Bistable regime for a system with trait values taken from a uniform distribution (Refer to Figure 3 for results from the Woodland regime) . We show how the initial trait distribution (shown with yellow bars) evolves for different initial values of grass cover (G). (A) For $\beta = 0.17$ which corresponds to the bistable regime when sapling resistance to fire θ is varied, we find grassland state with Initial $G = 0.9$ and therefore there is no tree cover present, while for other values of initial G, the steady-state distribution changes. (B) For $\beta = 0.3$ which corresponds to the bistable regime when sapling death rate μ is varied, we find the system in a savanna state for initial $G \geq 0.5$ and in each case only the sapling and trees with the least death rate survive.
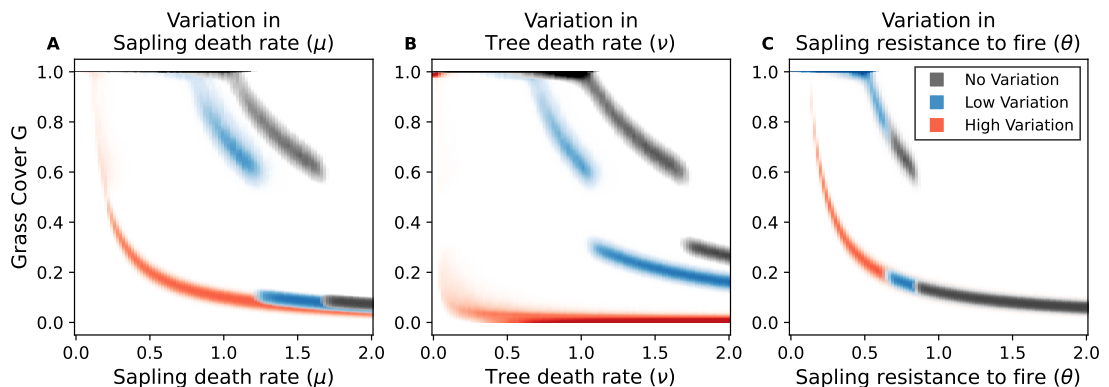

Supplementary Figure S8. Ecosystem properties follow similar trends in a stochastic model with continuous trait variations. With increasing trait variation, extent of grassland reduces, while that of woodland increases. The extent of the bistable region naturally shrinks due to stochasticity, and we cannot comment on that aspect. However, the quantum of jump in the abrupt shift decreases as trait variation is increased to a high value. Only one trait has variations at any instance. Parameters: The trait of interest is 0.5 for no variation, varies between 0.4–0.7 for low variation and between 0–1 for high variation. (A) sapling resistance to fire $\theta = 0.5$ and tree death rate $\nu = 0.1$. (B) $\theta = 0.5$ and sapling death rate $\mu = 0.05$ (C) $\nu = 0.1$ and $\mu = 0.2$.

Supplementary Figure S9. Population dynamics shows similar trends in a stochastic model and depends on population size. We show how the trait distribution changes over the course of the simulation when started from a uniform distribution with a high variation (Row 0, A0-C0). The results are qualitatively similar to that of the deterministic model with discrete traits. (Row 1) At the steady state of each simulation, there is usually only one trait value left in the population. That is, the population becomes monomorphic. To understand what the possible values for this steady state trait, we to perform an ensemble of simulations and plot their distribution (Rows 2-3). (A1-A3) The sapling death rate μ shifts towards to left ie. to lower values during the simulation. The final distribution of traits is highly concentrated close to the minimum value in the initial distribution. (B1-B3) The distribution of the tree death rate ν also shows a very similar behaviour as that of μ. (C1-C3) For the variation in sapling resistance to fire θ, the grass cover G was set to 0.6. The simulations in Row 2 were done for a population size of $N = 1000$, while in Row 3, the population size was $N = 400$. As the population size is decreased, the final trait distribution is more spread out in the case of μ (A3) and ν (B3).

Supplementary Figure S10. Population-level dynamics of the trait distributions of the sapling resistance to fire θ for different initial values for the grass cover G. The initial distribution of traits is a uniform distribution with high trait variation as shown in Row 1. This effect of initial conditions is similar to that of the deterministic model with discrete traits as shown in Fig. 3 C1-C3.
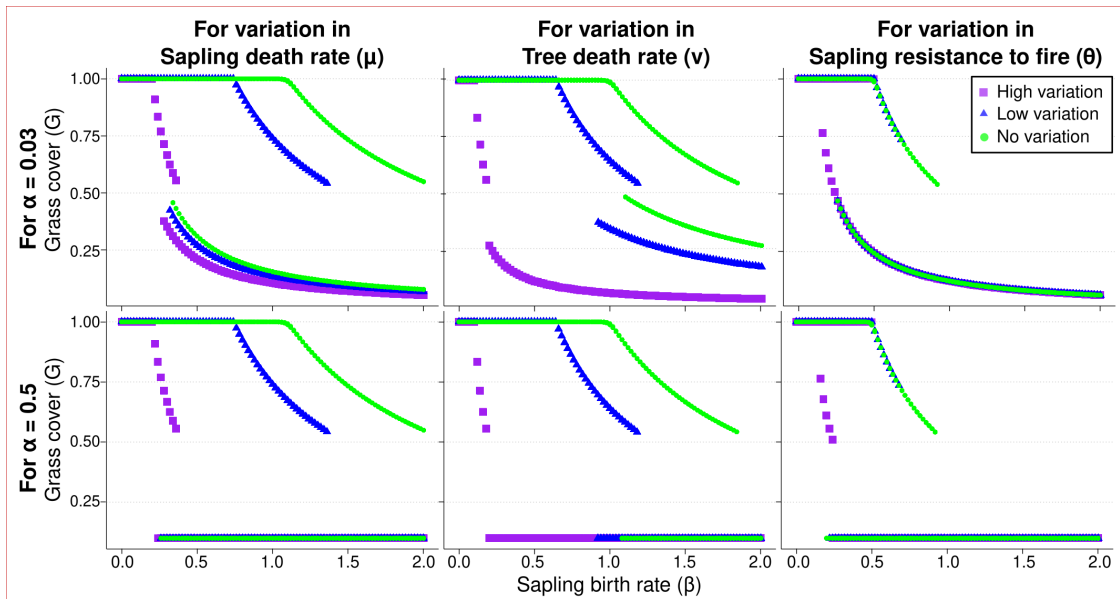
Supplementary Figure S11. Bifurcation diagrams (Grass cover vs Sapling birth rate) for a model including forest trees based on (Staver and Levin, 2012) while incorporating trait variations. The forest trees essentially function as an invasive organism which competitively exclude all the other kinds of vegetation. The bifurcation diagram with respect to beta follows different regimes as per the value of the competitive exclusion parameter α.0 For most of the range of α (shown here are bifurcation diagrams for $\alpha = 0.5$, there exists no woodland state, there is a grassland state which undergoes a pitchfork bifurcation at a certain critical value of β to become a savanna while at a lower value of β, the invasion by forest trees becomes stable. the bistable regime consists of the 'high grass cover' (grassland/savanna) and the 'low grass cover' (forest) state. It is to be noted that the value of forest cover is not a constant but a function of α and ϕ. At very low values of α (shown here are bifurcation diagrams for $\alpha = 0.03$, the invasion by forest trees is never stable and the bistability is between a grassland which transitions into a savanna as before and a woodland state with coexistence of grass, savanna saplings and savanna trees. The limiting case $\alpha \approx 0$ corresponds to the model described in the main text. The results for the extent of bistable regime and jump are in good agreement with those in the main text for all the cases of α, with an increase in trait variation corresponding to a lower extent of bistability.
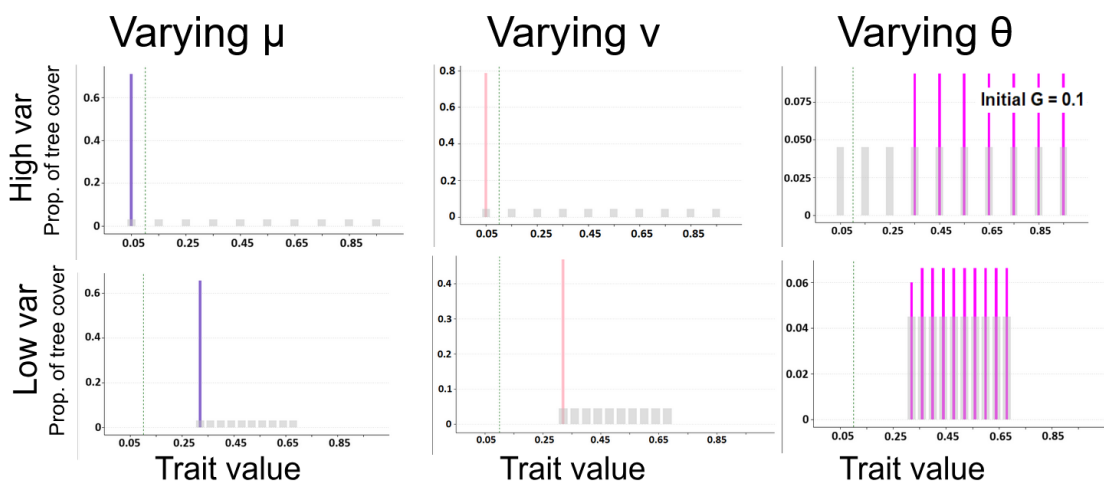
Supplementary Figure S12. Individual proportions of tree types for the model incorporating forest trees while incorporating trait variations. This agrees with the main model where in case of varying μ and ν results, with only the fittest type surviving for both high and low variation cases in both savanna and grassland states, while for varying θ we see survival of all types above a certain threshold.